Proceedings of the 33rd European Safety and Reliability Conference (ESREL 2023)
Edited by Mário P. Brito, Terje Aven, Piero Baraldi, Marko Čepin and Enrico Zio
 Published by Research Publishing, Singapore.
doi: 10.3850/978-981-18-8071-1_P055-cd

Identifying Changes in Degradation Stages for an Unsupervised Fault Prognosis Method for Engineering Systems

Miguel Angelo de Carvalho Michalski

Department of Mechatronics and Mechanical Systems, University of São Paulo, Brazil. E-mail: michalski@usp.br

Arthur Henrique de Andrade Melani

Department of Mechatronics and Mechanical Systems, University of São Paulo, Brazil. E-mail: melani@usp.br

Renan Favarão da Silva

Department of Mechatronics and Mechanical Systems, University of São Paulo, Brazil. E-mail: renanfavarao@usp.br

Gilberto Francisco Martha de Souza

Department of Mechatronics and Mechanical Systems, University of São Paulo, Brazil. E-mail: gfmsouza@usp.br

The maintenance strategy known as Condition-Based Maintenance (CBM) has become increasingly popular as it optimizes asset availability by minimizing maintenance downtimes and reducing overall maintenance costs. To do so, it analyses asset monitoring data to forecast the degradation and prevent failure before it occurs, a process called fault prognosis. This process generally comprises four basic steps: data acquisition, construction of a Health Indicator (HI), identification of the Health Stages (HS), and prediction of the Remaining Useful Life (RUL). Nevertheless, it is usually dependent on prior knowledge of a failure threshold, thus enabling the prediction of the RUL. In cases where this information is not available, a different prognosis approach is required. Therefore, rather than predicting the RUL, the proposed method intends to indicate the proximity of the failure occurrence based on the premise that during the development of the fault, breakpoints associated with the acceleration of the degradation rate occur. In this way, evaluating only the HI behavior, without considering previously monitored data, the proposed method could be applied to machines whose faults of interest had not yet been observed. To validate the method, it is applied to synthetically generated HI data with different behaviors over time. Results show that the method has the potential to be used in scenarios where there is no previous information on the degradation pattern.

Keywords: Fault prognosis, unsupervised prognosis, ARIMA, adaptive prognosis, CBM.

1. Introduction

Condition-Based Maintenance (CBM) is a maintenance strategy based on the real-time diagnosis of impending failures and the prognosis of future equipment health (Peng et al. 2010). Using predictive techniques, monitoring and follow-up of the condition parameters are carried out to identify the need for equipment maintenance (da Silva and de Souza 2022). Therefore, by employing this proactive strategy, organizations can enhance physical asset availability and reduce maintenance costs, which has led to a significant increase in the popularity of CBM in recent years.

Fault detection, diagnosis, and prognosis are the key processes to implementing the CBM strategy. After detecting and diagnosing a failure mode, its degradation shall be tracked to predict how long the system can be operating before failure. Thus, fault prognosis allows for the prediction of failure occurrence and the components' Remaining Useful Life (RUL), thereby enabling timely and cost-effective maintenance decisions (de Souza et al. 2021).

The degradation trend of a given component can be divided into multiple stages, and each stage

has uncertain changes (Liu and Fan 2022) that can be evaluated with the support of machine learning and statistical modeling for prognosis. Changing from one degradation stage to another indicates closer proximity to a failure, as shown in Fig. 1. The ability to accurately identify these changes is essential for ensuring the reliability, safety, and optimal performance of engineering systems.

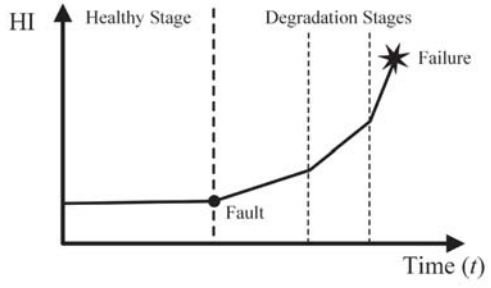

Fig. 1. Conceptual representation of a Health Indicator and its stages.

As seen in Fig. 1, the degradation trend of a given system can be observed by a Health Indicator (HI). Thus, HI represents the damage degree of said system computed by monitoring signals (Lei *et al.*, 2018).

The growing interest in fault prognosis methods has led to the development of various techniques, including data-driven, model-based, and hybrid approaches. These methods have been successfully applied to the aforementioned multi-stage degradation patterns, as reported by several authors (Guan *et al.* 2022; Liu *et al.* 2022; Liu and Fan 2022; Suzuki and Ito 2022; Wang *et al.* 2021; Wen *et al.* 2017; Yan *et al.* 2021).

Despite the promising advancements in fault prognosis methods, a major drawback of the approaches presented in the literature is their reliance on supervised learning techniques. Supervised methods require substantial amounts of labeled data, which can be challenging to obtain, particularly for complex engineering systems. The process of collecting and annotating such data is time-consuming, labor-intensive, and often expensive, as it requires expert knowledge to accurately label the degradation stages and fault conditions. Additionally, these methods cannot be applied in scenarios where the studied failure has not occurred or has not been properly monitored throughout its degradation phase.

In this context, this paper proposes a method to identify changes in the degradation stages for an unsupervised faults prognosis. The proposed method is based on the following premises:

- Prognosis is the capability to use available observations to predict upcoming states of machines or forecast the failure before it occurs (Tung and Yang, 2009). This implies that fault prognosis is not limited to estimating RUL
- Degradation stage changes could be used to determine the approximation of a failure
- The method only applies after the detection and diagnosis of a given failure mode
- The system under study has no labelled monitoring data related to the failure mode
- There is no knowledge regarding either failure thresholds or the system End-of-Life (EoL)
- The health indicator shall have at least three stages (healthy, initial degradation, and critical degradation)
- The focus of the method is the prevention and mitigation of the risk associated with a failure occurrence

Accordingly, the proposed method identifies the approximation of the failure from a change in the degradation stage. To demonstrate the method, synthetic data from six distinct patterns of HIs has been utilized.

These datasets have been implemented to illustrate how alterations within the degradation pattern may be identified. Such changes indicate that the equipment's degradation is accelerating, which implies that a failure is more likely to occur. The results demonstrate that, given certain conditions, the method exhibits robust and reliable performance, indicating the potential for its application in real engineering systems.

The remainder of this article is structured as follows: Section 2 presents the proposed unsupervised method, followed by examples of its application in Section 3, where its strengths and limitations are highlighted and discussed. Finally, Section 4 presents the conclusions of this work.

2. Proposed Method

The method proposed in this work comprises four consecutive processes, as shown in Fig. 2. Some prior assumptions are considered, such as the pre-

existence of an HI, which may be a Physical HI (PHI) or a Virtual HI (VHI) (Lei *et al*. 2018). Additionally, it is assumed that the fault has already been detected, and the HI can be observed from the moment of detection onward.

Also, it should be noted that the proposed method applies only to cases where the degradation process of the failure mode considered has multiple Health Stages (HS), with the first being the healthy state, followed by at least one degradation state and one critical state (Lei *et al*. 2018).

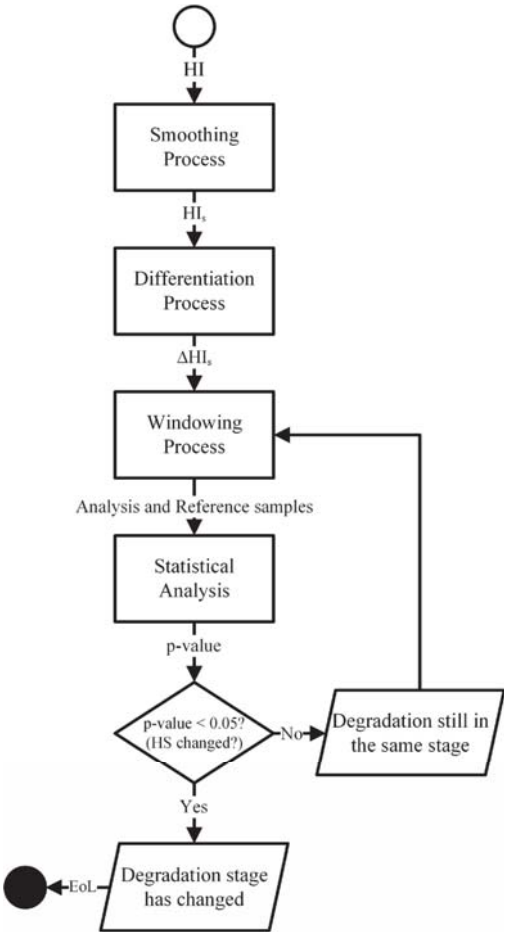

Fig. 2. Proposed method for unsupervised prognosis.

The first step of the proposed method is the HI smoothing process. The purpose of this step is to remove noise from the HI, highlighting its trend and resulting in a smoothed HI (HI_s). Since smoothing methods tend to work as low-pass filters, thereby affecting high-frequency noise more than low-frequency noise, an additive decomposition method was chosen for this process.

Accordingly, the smoothing process is based on ARIMA models, which are often represented as ARIMA (p, d, q), where p is the number of autoregressive components, q is the number of moving average components, and d is the number of times the original series is differentiated (Michalski *et al*. 2022). The values of p, d, and q are selected for each analysis conducted based on the Hyndman-Khandakar algorithm (Hyndman and Khandakar 2008).

The Hyndman-Khandakar algorithm-based ARIMA method demonstrated greater suitability than other tested approaches such as cubic spline smoothing, Moving Average (MA), Cumulative Sum (CUSUM) control chart, and local polynomial regression fitting, specifically the Locally Estimated Scatterplot Smoothing (LOESS) and Locally Weighted Scatterplot Smoothing (LOWESS) methods, for HI smoothing for two primary reasons. Firstly, the applied smoothing method does not require any hyperparameter definition, rendering it entirely unsupervised and, secondly, the results obtained with this method maintain the necessary dispersion for statistical analysis while reducing the noise level to a more appropriate level.

The second step of the method involves the differentiation of HI_s, intending to create a stationary signal. The result of this process is the ΔHI_s, given by Eq. (1).

$$\Delta HI_s(t) = HI_s(t) - HI_s(t-1) \quad (1)$$

It is worth noting that both the smoothing and differentiation processes are performed in a single batch, i.e., all the observations available are considered in each analysis. Besides, as shown in Eq. (1), the time series of the ΔHI_s has one less observation compared to the HI and HI_s series, i.e., for an HI with n observations, the correspondent ΔHI_s will have (n–1) observations.

In the third step, the windowing process prepares the analysis and reference samples for statistical analysis. In this step, a size for the analysis window, w, must be defined, which is the only hyperparameter required by the method. For better comprehension, Fig. 3 illustrates how the windowing process works when analyzing an HI with a time series containing 9 observations (n = 9 and an analysis window with 3 observations (w =

3). Each observation is represented by a numbered square.

As depicted in Fig. 3, it is required that $n \geq (w + 2)$ for the first analysis to avoid complete overlap between the analysis and reference samples. During the windowing process, the analysis and reference samples have the same size, w, until the analysis of the $(2w + 1)$ observation. From the subsequent observation, the reference sample starts to incrementally increase with each new observation considered.

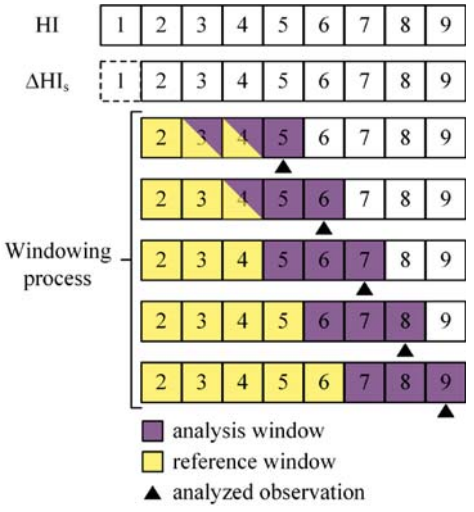

Fig. 3. Graphic representation of the windowing process for a HI with $n = 9$ and $w = 3$.

Then, in the fourth step of the method, each pair of samples generated in the windowing process is subjected to statistical analysis to determine whether the sample means are statistically equivalent (null hypothesis) or not. Given that the variance between the two samples is assumed to be different and the number of observations in each sample varies during the application of the method, Welch's t-test (Welch. 1947) was selected to perform this comparison.

As long as the p-value obtained from the test remains above the established limit value (based on a selected confidence level), the null hypothesis is accepted. In this case, the analysis sample is shifted forward, allowing for continuous monitoring of the system's behavior. However, if the p-value is consistently below its threshold in subsequent analyses, degradation is no longer in the same HS. This is considered to determine the EoL of the system in terms of reliability and risk in an unsupervised fault prognosis.

3. Method Application Examples

To demonstrate the application of the proposed method and discuss its strengths and limitations, six synthetically generated HIs with different pattern behavior over time are considered. In these application examples, The HIs are not related to any specific system and are represented as time series of dimensionless values that are generated from mathematical functions.

Two fundamental degradation patterns were considered to construct the HI for each case: linear and exponential. Hence, for four out of the six cases, the HI is built by combining these two patterns. In the remaining two cases, only one of the two patterns is taken into consideration, resulting in the absence of a defined breakpoint.

Fig. 4 schematically presents the combined patterns considered, where α, β, and θ are the degradation rates of each HS. Furthermore, in all cases, an error ε was considered, with $\varepsilon \sim N(0, \sigma^2)$, added to the HI for each observation. The HI parameters considered in each case are shown in Table 1. The difference between cases 1 and 3 and between cases 2 and 4 is only the noise level considered, expressed by its variance σ^2.

.

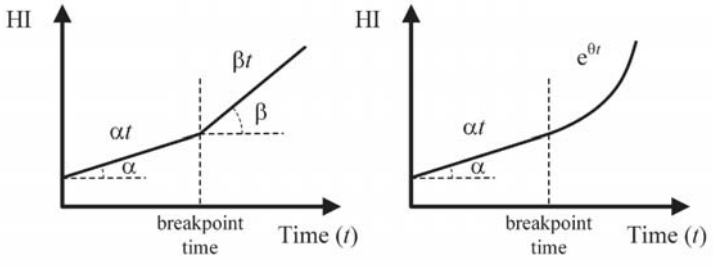

Fig. 4. Schematic representation of the combined degradation patterns considered.

Table 1. HI parameters for each case.

Case	Degradation pattern	α	β	θ	σ^2	Breakpoint Time
1	linear + linear	0.0155	0.0425	-	3.50	500
2	linear + exponential	0.0045	-	0.0065	3.50	500
3	linear + linear	0.0155	0.0425	-	0.10	500
4	linear + exponential	0.0045	-	0.0065	0.10	500
5	linear	0.0285	-	-	1.25	-
6	exponential	-	-	0.0034	1.25	-

To ensure consistency in comparing the results obtained with different cases, the initial HI value was set at approximately 50, reaching a value of approximately 80 after 1,000 observations in all cases. Fig. 5 presents the simulated HI values for each case over time

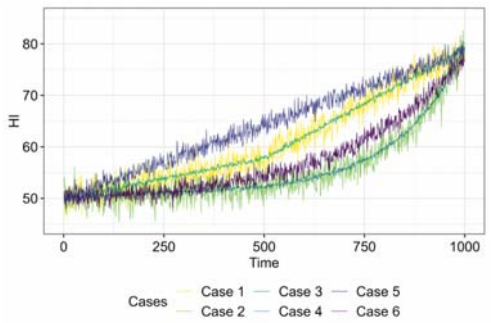

Fig. 5. Simulated HI values for each case over time.

Once the HI is obtained the first step consists of smoothing the HI from the construction of an ARIMA model for the considered data. Fig. 6 presents the results for the six cases considered.

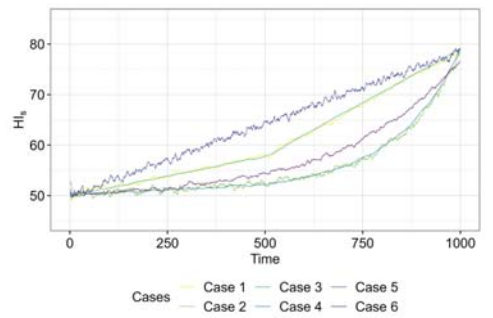

Fig. 6. Smoothed HI (HI_s) for each case over time.

A unique ARIMA model is derived for each case studied since the model is chosen for each analysis performed. Note that the influence of the HI noise level on the smoothing process is evident, despite the generation of a tailored model for each case.

The next step is to perform the differentiation process, obtaining in this way the ΔHI_s for each case, as presented in Fig. 7.

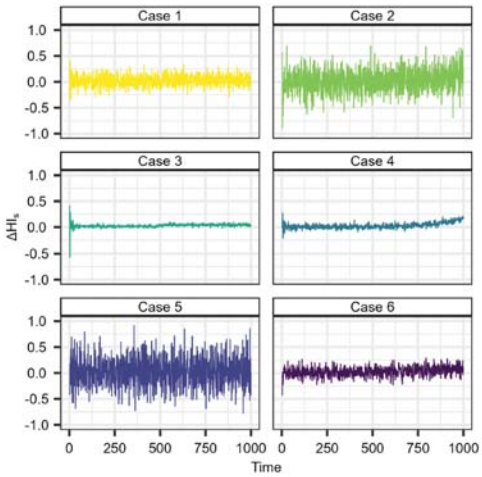

Fig. 7. ΔHI_s for each case over time.

The following steps include the statistical analysis of the ΔHI_s obtained through the presented windowing process, and subsequently, the evaluation of the p-value obtained from Welch's test. This test assesses the average of the two samples (reference sample and analysis sample) for each observation.

Fig. 8 presents the p-values obtained from Welch's test over time for each case, using an analysis window of 100 observations and a confidence level of 95%. The black dashed line represents the established threshold indicating that the null hypothesis of the mean values of the analysis and reference samples being statistically different is rejected.

The results show that the best outcomes were achieved in cases 3 and 4, in which the p-

value presents two distinct patterns: the p-value remains close to the maximum value before the HI breakpoint and then decreases shortly after the defined breakpoint. The value then remains constant below the pre-established threshold (0.05, in this study), indicating that the mean value of the analysis sample differs statistically from that of the reference sample.

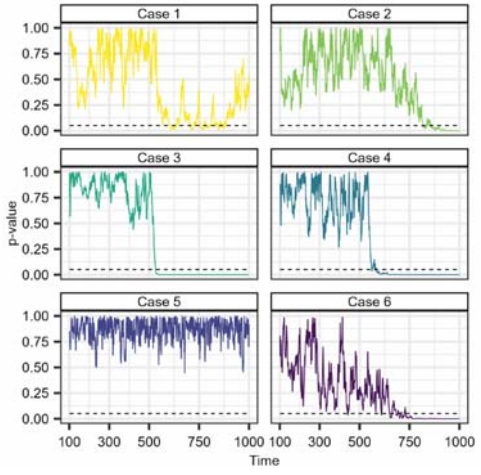

Fig. 8. Welch's test p-values over time for each case considering an analysis window of 100 observations.

In case 1, the p-value is not consistently below the threshold after the breakpoint time, unlike case 3. Conversely, case 2 exhibits a slower transition between the maximum and minimum p-values compared to case 4, although the p-value stabilizes below the defined threshold after several observations. The disparity in the response between cases 1 and 3, and cases 2 and 4, can be solely attributed to the higher level of noise added to the HI in cases 1 and 2.

Finally, cases 5 and 6 display different result patterns compared to the other cases. Case 5 shows a single pattern of linear degradation and does not exhibit the anticipated two distinct patterns. On the other hand, case 6 demonstrates a constant downward trend between the maximum and minimum p-values. This indicates that the mean values of subsequent analysis samples and their corresponding reference samples gradually increase in distance. This increase is associated with the degradation pattern following a single exponential curve in this case.

Apart from examining the impact of degradation patterns and HI noise levels, two additional factors that could influence the results of the method are worth exploring: the size of the analysis window (the only hyperparameter of the method), and the distance between the breakpoint and the last analyzed observation.

Regarding the former, Figs. 9 and 10 exhibit the obtained outcomes for an analysis window of 50 and 200 observations, respectively. It is important to note that using smaller windows enhances the method's sensitivity to the influence of noise on HI, while larger windows have the opposite effect of reducing this sensitivity.

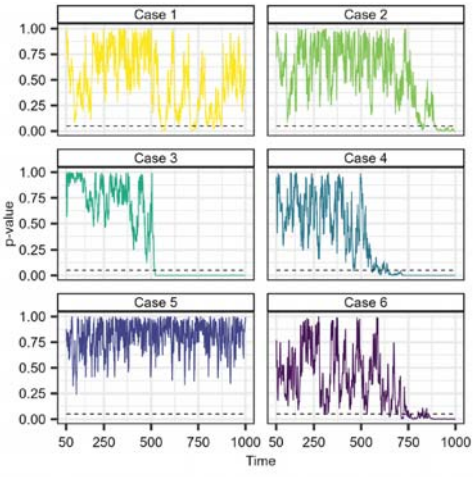

Fig. 9. Welch's test p-values over time for each case considering an analysis window of 50 observations.

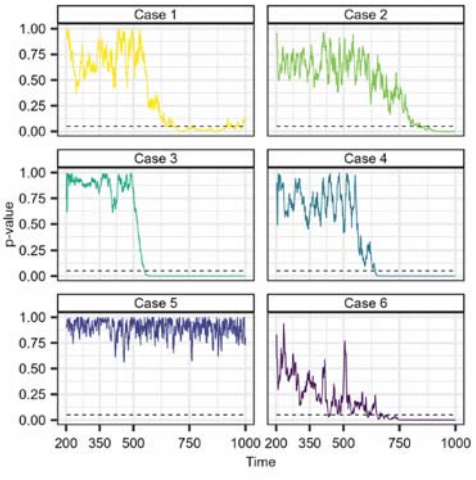

Fig. 10. Welch's test p-values over time for each case considering an analysis window of 200 observations.

Concerning the distance between the breakpoint and the last observation analyzed, the results obtained by considering only the first 500, 550, and 600 observations are presented in Fig. 11, Fig. 12, and Fig. 13, respectively. These results were obtained using an analysis window consisting of 100 observations.

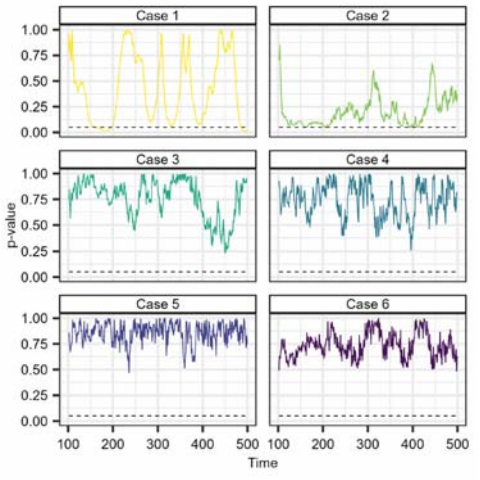

Fig. 11. Welch's test p-values over time for each case considering the first 500 observations and an analysis window of 100 observations.

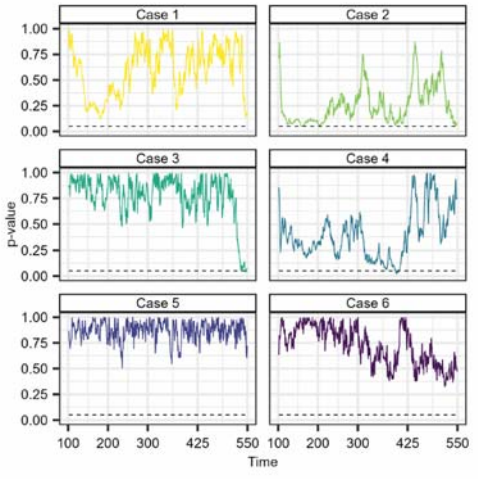

Fig. 12. Welch's test p-values over time for each case considering the first 550 observations and an analysis window of 100 observations.

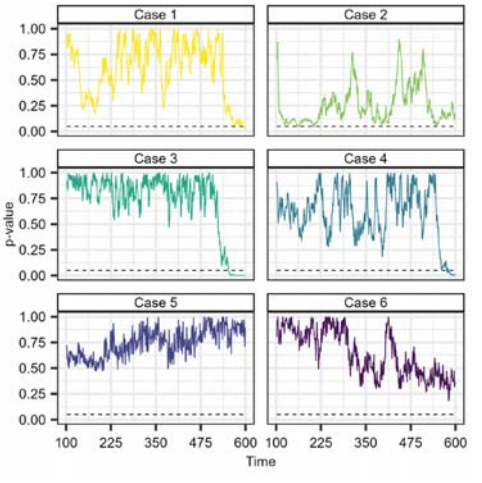

Fig. 13. Welch's test p-values over time for each case considering the first 600 observations and an analysis window of 100 observations.

The graphs demonstrate how the inclusion of observations obtained after the breakpoint affects the p-value outcomes. Notably, in cases 1, 3, and 4, this effect is particularly significant. In cases 1 and 4, with 100 observations after the breakpoint, it would already be feasible to determine a change in the system's degradation pattern. For case 3, in turn, a change could be detected with just 50 observations after the breakpoint.

Furthermore, since the smoothing process is executed in a single block, considering all available observations, it is anticipated that the p-value response will fluctuate depending on the number of observations considered. This underscores the importance of consistently monitoring the degradation process of the system and applying the method accordingly.

4. Conclusions

The objective of this work is to present and explore a method capable of performing unsupervised fault prognosis for engineering systems by detecting changes in the degradation pattern, i.e., changes in HS after fault detection. Accordingly, its application is recommended especially in cases where the failure history has not yet been established and the available knowledge about the failure threshold is limited.

From six different cases, it was possible to demonstrate that, overall, the proposed method

presents encouraging results. In certain scenarios, the method proves to be effective in detecting a change in the degradation pattern within a few observations after the breakpoint. For example, conditions where the degradation trend is linear and the HI has low noise levels are more favorable for accurately identifying the breakpoint. In these instances, it may even be possible to establish an EoL threshold based on the p-value, which is associated with an increased risk of imminent failure.

Further studies of the method are still necessary, including verification under different scenarios beyond those considered in this work and a better evaluation of its limitations. Nevertheless, while there is still much work to be done, this study demonstrates the potential of an adaptive prognostic method as a supporting process for CBM and encourages its practical application in real-world scenarios soon.

Acknowledgment

The authors thank the financial support of FDTE (Fundação para o Desenvolvimento Tecnológico da Engenharia), and FUSP (Fundação de Apoio à Universidade de São Paulo) during the development of the present research.

References

da Silva, R.F., de Souza, G.F.M. (2022). Modeling a maintenance management framework for asset management based on ISO 55000 series guidelines. *Journal of Quality in Maintenance Engineering 28(4),* 915-937.

de Souza, G.F.M., Netto, A.C., Melani, A.H.A., Michalski, M.A.C., da Silva, R.F. (2021). *Reliability Analysis and Asset Management of Engineering Systems* (1st ed.). Elsevier.

Guan, Q., Wei, X., Bai, W., Jia, L. (2022). Two-stage degradation modeling for remaining useful life prediction based on the Wiener process with measurement errors. *Quality and Reliability Engineering International 38(7)*, 3485–3512.

Hyndman, R.J., Khandakar, Y. (2008). Automatic Time Series Forecasting: The forecast Package for R. *Journal of Statistical Software 27(3)*, 1–22.

Lei, Y., Li, N., Guo, L., Li, N., Yan, T., Lin, J. (2018). Machinery health prognostics: A systematic review from data acquisition to RUL prediction. *Mechanical Systems and Signal Processing 104*, 799–834.

Liu, S., Fan, L. (2022). An adaptative prediction approach for rolling bearing remaining useful life based on multistage model with three-source variability. *Reliability Engineering and System Safety 218,* 108182.

Liu, J., Yu, Z., Zuo, H., Fu, R., Feng, X. (2022). Multi-stage residual life prediction of aero-engine based on real-time clustering and combined prediction model. *Reliability Engineering and System Safety 225*, 108624.

Michalski, M.A.C., Melani, A.H.A., da Silva, R.F., de Souza, G.F.M. (2022). Remaining Useful Life Estimation Based on an Adaptive Approach of Autoregressive Integrated Moving Average (ARIMA). In: Leva, M.C., Patelli, E., Podofillini, L., Wilson, S. (Eds.), *Proceedings of the 32nd European Safety and Reliability Conference (ESREL 2022)*. Research Publishing, Singapore, Dublin, Ireland, 1227–1234.

Peng, Y., Dong, M., Zuo, M.J. (2010). Current status of machine prognostics in condition-based maintenance: a review. *The International Journal of Advanced Manufacturing Technology 50,* 297-313.

Suzuki, M., Ito, M. (2022). Maintenance scheduling of nuclear components under reliability constraints using adaptive parallel particle swarm optimization. *Journal of Advanced Mechanical Design, Systems, and Manufacturing 16(4)*.

Tung, T.V., Yang, B.S. (2009) Machine Fault Diagnosis and Prognosis: The State of The Art. *International Journal of Fluid Machinery and Systems 2 (1),* 61–71.

Wang, J., Han, X., Zhang, Y., Bai, G. (2021). Modeling the varying effects of shocks for a multi-stage degradation process. *Reliability Engineering and System Safety 215*, 107925.

Welch, B.L. (1947). The Generalization of 'Student's' Problem when Several Different Population Variances are Involved. *Biometrika 34 (1/2)*, 28–35.

Wen, Y., Wu, J., Yuan, Y. (2017). Multiple-phase modeling of degradation signal for condition monitoring and remaining useful life prediction. *IEEE Transactions on Reliability 66(3)*, 924–938.

Yan, H., Zuo, H., Sun, J., Zhou, D., Wang, H. (2021). Two-Stage Degradation Assessment and Prediction Method for Aircraft Engine Based on Data Fusion. *International Journal of Aerospace Engineering 2021.*